Corrigendum

BENJAMIN A. SCHENKEL,[a,b,c] ROGER EDWARDS,[d] AND MICHAEL CONIGLIO[c]

[a] *Cooperative Institute for Mesoscale Meteorological Studies, University of Oklahoma, Norman, Oklahoma*
[b] *School of Meteorology, University of Oklahoma, Norman, Oklahoma*
[c] *NOAA/NSSL, Norman, Oklahoma*
[d] *NOAA/SPC, Norman, Oklahoma*

(Manuscript received 13 April 2021, in final form 30 April 2021)

An error was discovered in the inadvertent inclusion of tropical cyclone (TC) motion from both the composite hodographs (Fig. 12) and vertical profiles of TC-relative tangential and radial winds (Fig. 13) computed from radiosondes sampling landfalling TCs in Schenkel et al. (2020). There are two primary reasons why TC motion should have been removed from these figures. First, the inclusion of TC motion makes it impossible to determine whether changes in the total wind field are due to the ambient or TC wind field when Fig. 12 and especially Fig. 13 were focused on differences in the latter. Second, exclusion of TC motion is consistent with previous studies of TC tornadoes (McCaul 1991; Baker et al. 2009) and the response of the TC circulation to ambient deep-tropospheric vertical wind shear (VWS; Zhang et al. 2013; DeHart et al. 2014). The removal of TC motion shows that only the TC secondary circulation strengthens with increasing VWS, which contrasts with Schenkel et al. (2020) that incorrectly showed increases in both the TC primary and secondary circulation. More specific details on these changes to the conclusions and the revised versions of Figs. 12 and 13 are discussed below.

The removal of TC motion from the composite hodographs in Fig. 12 shows a shift in the hodographs with no changes to the overarching conclusions. However, these revisions to Fig. 12 enable more direct comparison with hodographs shown in prior studies of TC tornadoes where TC motion is removed (McCaul 1991; Baker et al. 2009).

In contrast to Fig. 12, the revised version of Fig. 13 shows that the TC secondary circulation, and not the primary circulation, statistically strengthens in the downshear quadrants and weakens in the upshear quadrants with increasing VWS. These results are consistent with previous work (Black et al. 2002; Molinari and Vollaro 2010). Focusing on the downshear-left and downshear-right quadrants, the radial wind speed more than doubles between the weak and strong VWS categories. Moreover, the largest magnitude changes occur between 250 and 500 m above the surface, especially in the downshear-right quadrant. It is this strengthening of the TC secondary circulation and the associated stronger convective-scale vertical wind shear that likely partially supports favorable kinematic environments for tornadoes as suggested by prior work (Molinari and Vollaro 2008, 2010). In the original manuscript, the constructive superposition between increasing north-northeastward TC motion associated with stronger VWS and the TC winds in the downshear-right quadrant (Corbosiero and Molinari 2003; Schenkel et al. 2020) provided the false impression that the primary circulation was strengthening in this quadrant. Instead, except for the upshear-left quadrant, the exclusion of TC motion in Fig. 13 shows no statistical changes in the TC primary circulation in any quadrant with increasing VWS.

Together, these changes do not alter the primary conclusions of the manuscript that VWS impacts both the frequency and location of TC tornadoes. Rather, this corrigendum shows changes in one potential physical explanation for how strong VWS provides favorable kinematic environments for TC tornadoes. Namely, only the secondary circulation (and not the primary circulation) strengthens with stronger VWS with increases that are beyond those shown in Schenkel et al. (2020). This larger enhancement of only the TC secondary circulation, and associated strengthening of convective-scale vertical wind shear, likely partially explains why kinematic environments in the downshear sectors more strongly support tornadoes as VWS increases.

Corresponding author: Benjamin A. Schenkel, benschenkel@gmail.com

DOI: 10.1175/WAF-D-21-0055.1

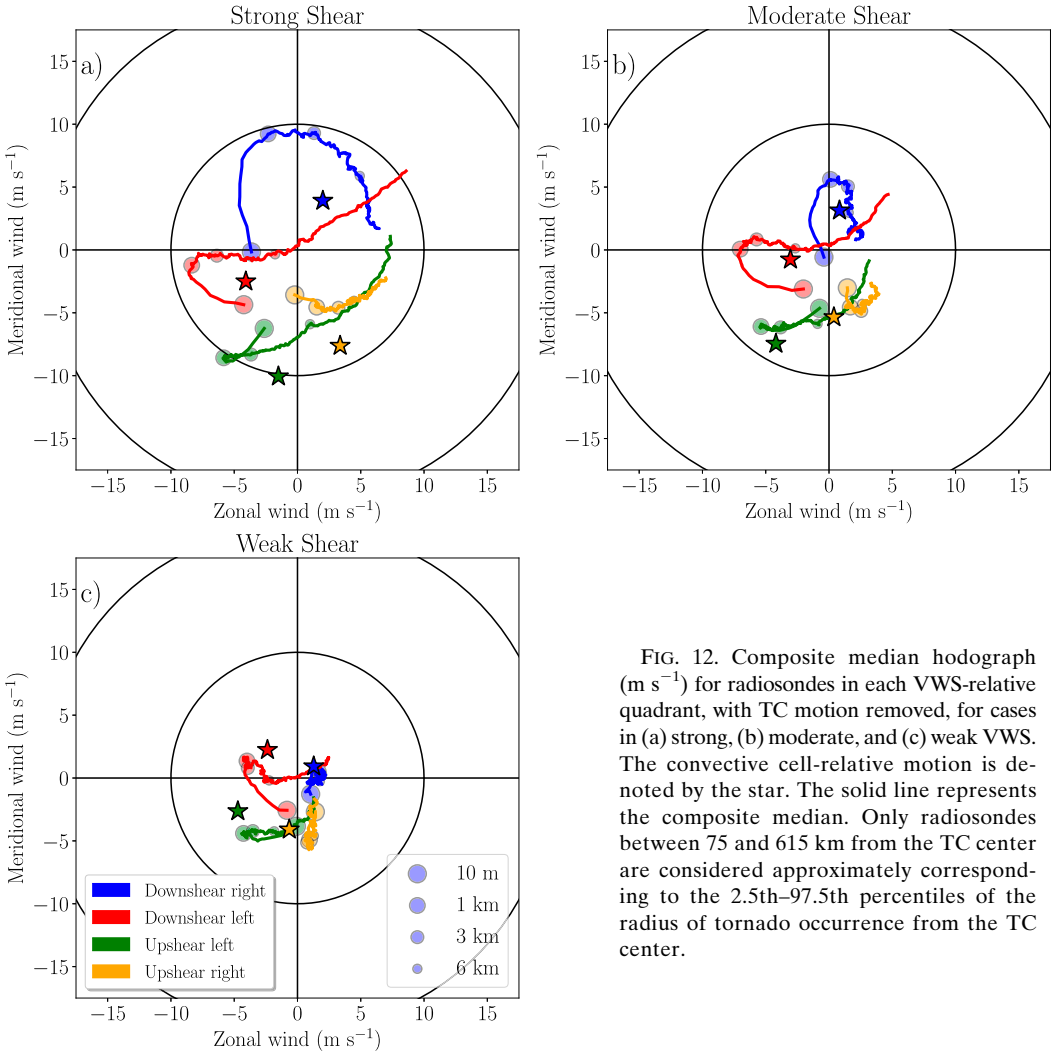

FIG. 12. Composite median hodograph (m s^{-1}) for radiosondes in each VWS-relative quadrant, with TC motion removed, for cases in (a) strong, (b) moderate, and (c) weak VWS. The convective cell-relative motion is denoted by the star. The solid line represents the composite median. Only radiosondes between 75 and 615 km from the TC center are considered approximately corresponding to the 2.5th–97.5th percentiles of the radius of tornado occurrence from the TC center.

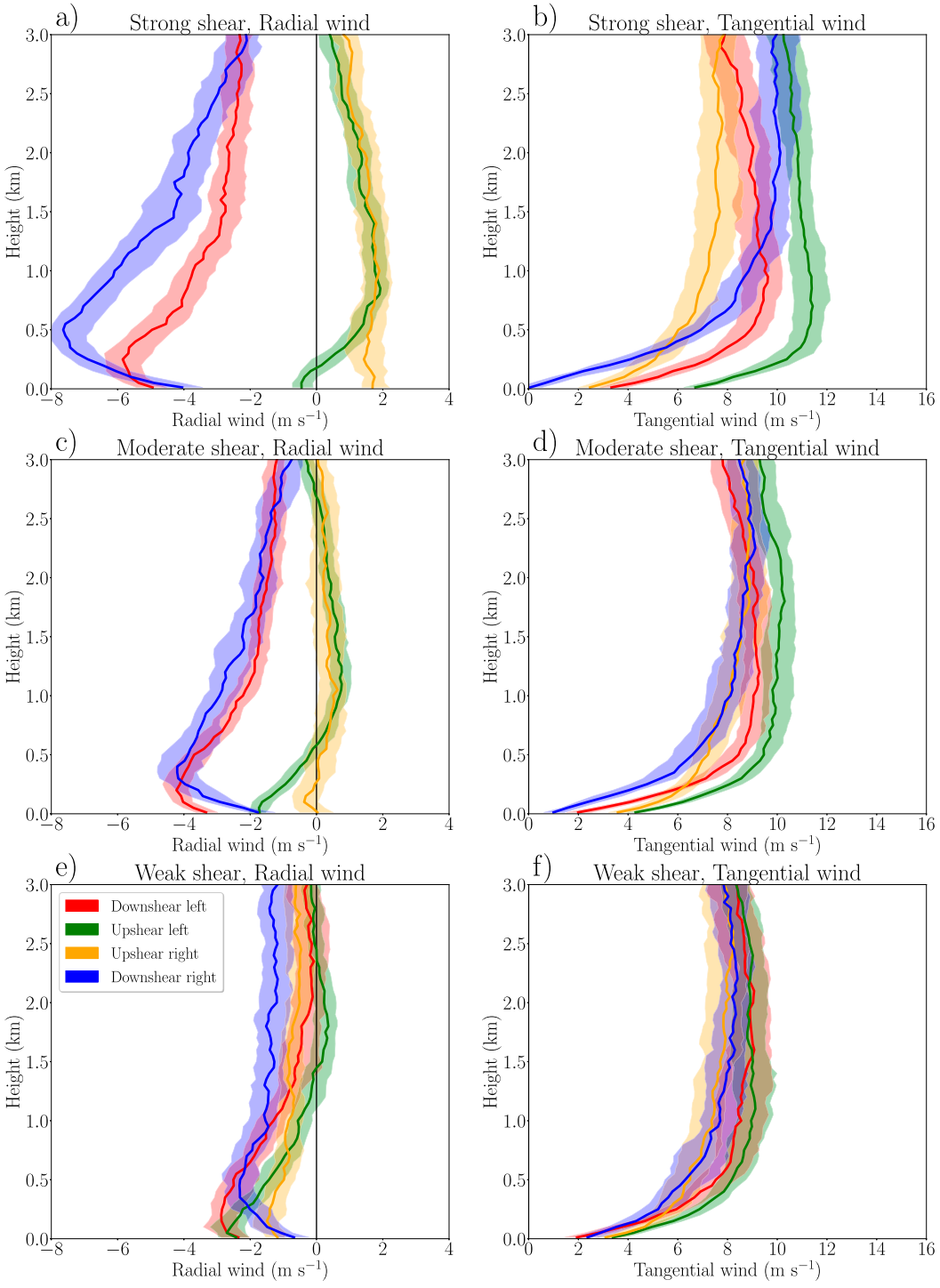

FIG. 13. Composite median (solid line) and its 95% confidence interval (shading) of vertical profiles of cyclone-relative radial wind (m s^{-1}) and tangential wind (m s^{-1}), with TC motion removed, computed from radiosondes in each of the VWS-relative quadrants for TCs in (a),(b) strong; (c),(d) moderate; and (e),(f) weak VWS. Only radiosondes between 75 and 615 km from the TC center are considered approximately corresponding to the 2.5th–97.5th percentiles of the radius of tornado occurrence from the TC center.

REFERENCES

Baker, A. K., M. D. Parker, and M. D. Eastin, 2009: Environmental ingredients for supercells and tornadoes within Hurricane Ivan. *Wea. Forecasting*, **24**, 223–244, https://doi.org/10.1175/2008WAF2222146.1.

Black, M., J. Gamache, F. Marks, C. Samsury, and H. Willoughby, 2002: Eastern Pacific Hurricanes Jimena of 1991 and Olivia of 1994: The effect of vertical shear on structure and intensity. *Mon. Wea. Rev.*, **130**, 2291–2312, https://doi.org/10.1175/1520-0493(2002)130<2291:EPHJOA>2.0.CO;2.

Corbosiero, K., and J. Molinari, 2003: The relationship between storm motion, vertical wind shear, and convective asymmetries in tropical cyclones. *J. Atmos. Sci.*, **60**, 366–376, https://doi.org/10.1175/1520-0469(2003)060<0366:TRBSMV>2.0.CO;2.

DeHart, J. C., R. A. Houze, and R. F. Rogers, 2014: Quadrant distribution of tropical cyclone inner-core kinematics in relation to environmental shear. *J. Atmos. Sci.*, **71**, 2713–2732, https://doi.org/10.1175/JAS-D-13-0298.1.

McCaul, E. W., 1991: Buoyancy and shear characteristics of hurricane–tornado environments. *Mon. Wea. Rev.*, **119**, 1954–1978, https://doi.org/10.1175/1520-0493(1991)119<1954:BASCOH>2.0.CO;2.

Molinari, J., and D. Vollaro, 2008: Extreme helicity and intense convective towers in Hurricane Bonnie. *Mon. Wea. Rev.*, **136**, 4355–4372, https://doi.org/10.1175/2008MWR2423.1.

——, and ——, 2010: Distribution of helicity, CAPE, and shear in tropical cyclones. *J. Atmos. Sci.*, **67**, 274–284, https://doi.org/10.1175/2009JAS3090.1.

Schenkel, B., R. Edwards, and M. Coniglio, 2020: A climatological analysis of ambient deep-tropospheric vertical wind shear impacts upon tornadic supercells in tropical cyclones. *Wea. Forecasting*, **35**, 2033–2059, https://doi.org/10.1175/WAF-D-19-0220.1.

Zhang, J. A., R. F. Rogers, P. D. Reasor, E. W. Uhlhorn, and F. D. Marks, 2013: Asymmetric hurricane boundary layer structure from dropsonde composites in relation to the environmental vertical wind shear. *Mon. Wea. Rev.*, **141**, 3968–3984, https://doi.org/10.1175/MWR-D-12-00335.1.